

# GESTROPHIC ADJUSTEMENT OF DENSITY FRONTS: what do we learn from recent laboratory experiments ?

A. Stegner , V.Mitkin<sup>1</sup>, V. Zeitlin

Laboratoire de Météorologie Dynamique (CNRS)  
24, Rue Lhomond 75005, Paris, France ([stegner@lmd.ens.fr](mailto:stegner@lmd.ens.fr))

T. Pichon

Unité de Mécanique (ENSTA)  
Chemin de la lumière, 91120 Palaiseau France

## Abstract :

*We present here a rapid review on recent laboratory investigations on geostrophic adjustment of density fronts. Several configurations were studied: warm core lens, cyclonic-anticyclonic PV patches and uniform PV front. The geostrophic adjustment is the first dynamical process which converts a significant fraction of the potential energy input of the atmosphere and the ocean into kinetic energy. According to the cases we studied we have shown that during this rapid adjustment toward a quasi-equilibrium state, an important part of the initial energy could be transferred to wave motion or dissipated by small-scale non-hydrostatic instabilities. A mean adjusted state is always reached after one or two inertial period. Even if a strong wave activity is present in the initial region of unbalance, the time-averaged mean flow could nevertheless be adjusted. We have shown that the wave modes frequency is concentrated around the inertial frequency. Besides, some anticyclonic structures may also exhibit sub-inertial oscillations.*

**Key-words : Geostrophic adjustment, inertial gravity waves, instability**

## 1 Introduction

. The geostrophic adjustment is the first dynamical process which converts a significant fraction of the potential energy input of the atmosphere and the ocean into kinetic energy. The first theoretical guidelines for solving geostrophic adjustment problems were proposed by Rossby (1938) in the framework of rotating shallow water fluid, for a review see Blumen (1972). It is assumed that the initial unbalanced state will evolve naturally toward a steady balanced state, geostrophic or cyclogeostrophic, satisfying mass and lagrangian conservation of potential vorticity (PV). This standard Rossby scenario conveniently avoids the time-dependent problem and predicts the final state. The energy of this predicted adjusted state is always less than the initial energy. Inertia-gravity waves, with zero PV, are then expected to carry the missing part of the energy away from the adjusted state. However, the time-dependent problem deals with the complex reversible-irreversible interactions between the waves and the mean flow and the time needed to reach an adjusted state (if any) is not well defined. Previous laboratory experiments have shown that the geostrophic adjustment is a rapid process (Ungarish et al. (2001); Bouruet-Aubertot and Linden (2002); Rubino and Brandt (2003); Thivolle-Cazat et al. (2005)). But very few studies investigated the characteristic time of this process especially when strong wave activity is present. Besides, this standard scenario and recent theoretical studies on nonlinear geostrophic adjustment (Kuo and Polvani (2000); Zeitlin, et al. (2003); Plougonwen and Zeitlin (2005)) didn't take into account the instabilities or the dissipative processes that may affect the final adjusted state in a real three-dimensional fluid.

In order to study both the small-scale dissipative process and the spectrum of the wave emission during the geostrophic adjustment we performed several laboratory experiments in rotating fluids based on lock released configurations. In a two-layer configuration, vertical

---

<sup>1</sup> Current affiliation : Institute for Problems in Mechanics RAS, Moscow, Russia ([mitkin@ipmnet.ru](mailto:mitkin@ipmnet.ru)).

boundaries (i.e. locks) are used to fix initial height (or density) steps in the upper layer. For such cases when there is no relative motion in the layers the initial PV field is precisely controlled by the layer thickness. If the release of the vertical walls is rapid enough, we could then follow the geostrophic adjustment of a well defined initial condition corresponding to discontinuous profiles of constant PV. The simplicity of the initial condition makes these experiments easily reproducible.

## 2 Experimental configurations

We study the adjustment process in four experimental configurations. The term warm-core lens is generally used for mesoscale vortices, which contain a finite volume of warm and light water, at the ocean surface. A simple experimental configuration leads to similar dynamical structure (Stegner *et al.* 2004). A fixed volume of buoyant water is initially confined within a bottomless cylinder of radius  $R_c$  on the top of a dense rotating fluid Fig.1 (a).

We used the term "PV patches" for localised positive or negative potential vorticity (PV) anomalies of constant values within a uniform layer. The "PV patch" model is the generalisation of the Rankine vortex (cylindrical vorticity patch) for a rotating shallow-water layer. It is the simplest description of potential vorticity front with no outcropping. The corresponding experimental configurations for anticyclonic and cyclonic "PV patches" are shown respectively in Fig.1 (b) and Fig.1 (c).

The geostrophic adjustment of a motionless horizontal density gradient generally leads to a baroclinic tilted front corresponding to a simplified model of synoptic atmospheric fronts. We use a three-layer setup to study the adjustment of an uniform PV front. Two upper fluid layers having different density  $\rho_1$  and  $\rho_2$ , but the same thickness  $H_1$ , are initially separated by a bottomless cylinder. If the upper layers have exactly the same thickness the initial PV distribution is uniform and have the same value inside ( $r < R_c$ ) and outside ( $r > R_c$ ) the cylinder (Fig.1 (d)).

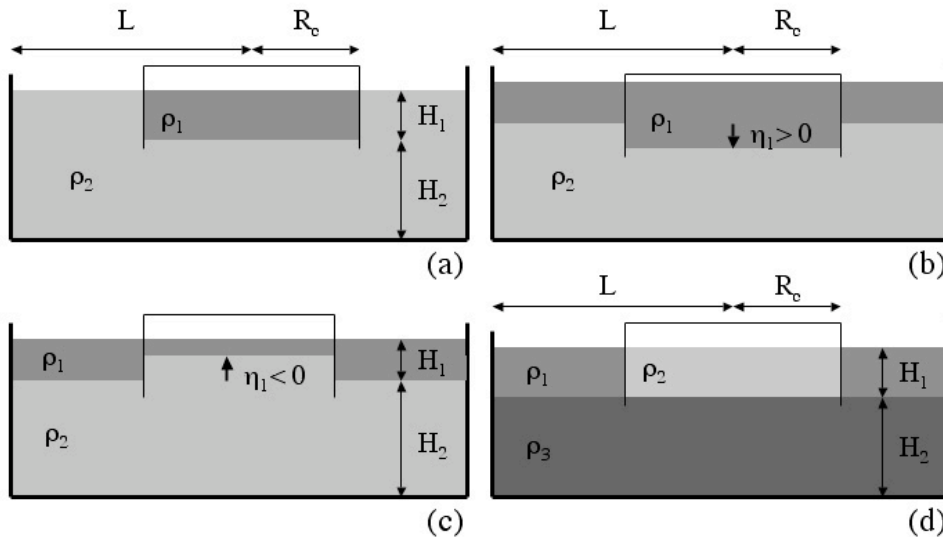


FIG. 1 – Initial experimental configuration for a “warm-core” lens (a), an anticyclonic (b) and a cyclonic (c) PV-patch and a uniform PV front (d).

For all the cases, according to the small thickness parameter  $\delta = H_1/H_2 \sim 0.1$  and the weak motion in the lower layer we assume that two upper layer follows the reduced-gravity rotating shallow-water (RSW) equations. The final adjusted state predicted by the standard Rossby

scenario is then fixed by the Burger number:  $Bu=(R_d/R_c)^2$  where  $R_d = \sqrt{g^* H_1} / 2\Omega_0$  is the internal deformation radius,  $g^*=(\rho_2-\rho_1)/\rho_2$  the reduced-gravity and the relative elevation parameter  $\lambda=\eta/H_1$  (configurations (b) and (c)).

Laser induced visualization (LIV) technique was used to measure with precision the upper fluid layer thickness along a line while standard particle image velocimetry (PIV) was used to measure the horizontal velocity field. Using simultaneously these two technique was the first attempt for direct and quantitative measurements of the potential vorticity field in rotating shallow-water layer experiments (Stegner, 2007).

### 3 Mean adjusted state

According to all the cases we studied, a mean adjusted state is reached after approximately one or two inertial period  $T_f$ . The rapidity of the geostrophic adjustment does not depends on the size (i.e.  $Bu$ ) or the amplitude (i.e.  $\lambda$ ) of the initial unbalance state. The so-called mean state is obtained from a simple time-averaging over  $T_f$ , in order to filter out the fast wave motion. We say that this averaged state reaches an equilibrium (i.e. get adjusted) when it's temporal evolution remain small in comparison with the characteristic wave frequency. Hence, even if a strong wave activity is present in the initial region of unbalance, the mean flow could nevertheless be adjusted. This experimental observation is in good agreement with the standard hypothesis of dynamical splitting between the fast and the slow component of motion. In the limit of small Rossby numbers, the asymptotic analysis shows that the slow component of motion doesn't feel the fast one (Zeitlin *et al.* 2003).

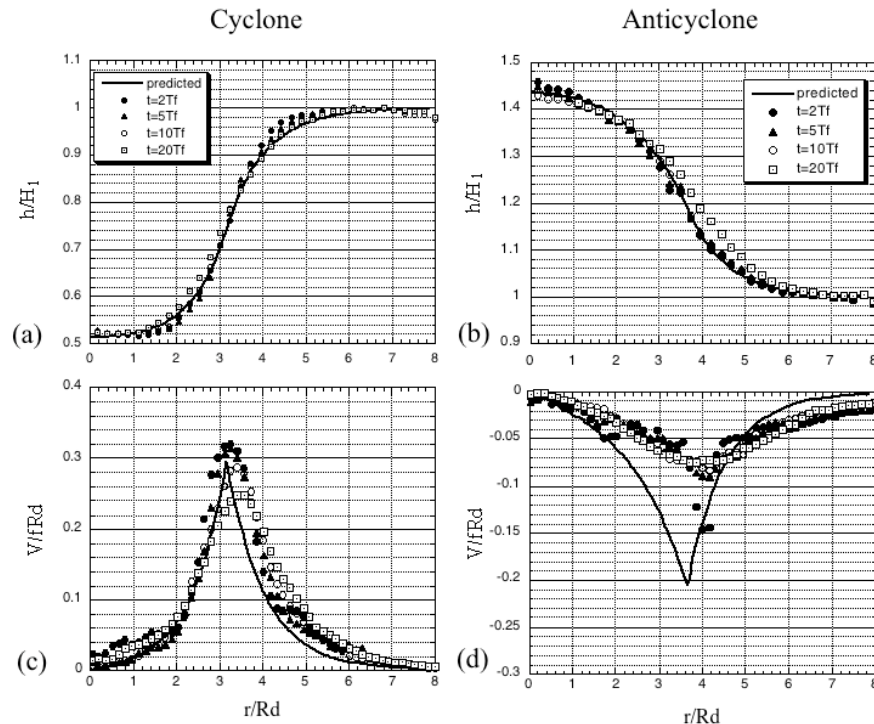


FIG. 2 –Mean averaged height (a,b) and velocity profiles (c,d) for anticyclonic and cyclonic PV-patches at various times. The solid lines correspond to the final states predicted by the standard adjustment scenario based on the lagrangian PVconservation (Stegner, 2007).

These two-layers or three-layers experiments show that the PV conservation remain robust even if the initial state does not satisfy the assumptions of the rotating shallow-water (RSW) model. Indeed, in almost all the cases, three-dimensional and non-hydrostatic motions (shocks or gravity current head) could occur in the early stage of adjustment. Nevertheless, the prediction of the RSW model based on the PV conservation gives a correct estimation of the mean adjusted state (Fig. 2). A very good agreement is found for the cases of cyclonic PV patch when there is no outcropping Fig. 2 (a,c). However, for the anticyclonic counterpart a significant dissipation of the kinetic energy occurs Fig.2 (d). Moreover, the PV conservation could be locally broken in the case of outcropping fronts when the initial PV profile exhibits a singularity (i.e. the layer thickness vanish at a given position).

#### 4 Inertial and sub-inertial wave activity

The relaxation of any unbalanced initial state in a rotating shallow-water model will always leads to the emission of Poincarre waves. According to our experiments and previous studies (Bouruet-Aubertot and Linden, 2002; Rubino and Brandt, 2003; Thivolle-Cazat *et al.*, 2005) the energy released to the wave modes during the adjustment is mainly concentrated around the inertial frequency. A significant wave activity remains for a long time (several inertial period) inside both the cyclonic and the anticyclonic structures even if the mean steady state is already adjusted Fig.2.

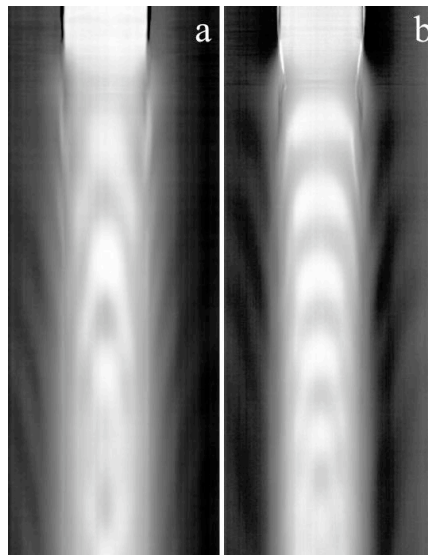


FIG. 3 – Spatio-temporal evolution of the upper layer relative oscillations for the cases of a anticyclonic (a) and a cyclonic (b) PV-patch.

The most striking results is a strong cyclone-anticyclone asymmetry in the wave frequency. According to the spatio-temporal plots, the oscillation is faster for the positive PV anomaly (Fig 3 (b)) in comparison with the negative PV anomaly (Fig 3 (a)). In the rotating shallow-water configuration, the apparition of sub-inertial modes ( $\omega/f < 1$ ) corresponds to trapped modes in other words, these modes must have an evanescent structure outside the PV-patch. If the relative vorticity is strong enough, a finite number of trapped modes could appear in anticyclonic vorticity region only (Plougonwen and Zeitlin, 2005). The present experiment shows, for the first time in laboratory, the existence of sub-inertial modes within an anticyclonic vortex.

## 5 Small-scale instabilities

For the warm core lens configuration, detailed analysis of the velocity field evolution show that strong and localized dissipation occurs in the very initial stage of adjustment ( $t < 2T_f$ ) while the flow experiences only a weak dissipation afterwards. This rapid dissipation, which occurs at the edge of the anticyclonic lenses, induces a significant deficit in the kinetic energy of the adjusted flow up to 50% or 80% (Stegner *et al.*, 2004). Dye visualization reveals that transient and rapid three-dimensional instabilities occur in the very first stage of adjustment. These three-dimensional instabilities localized in time (less than one inertial period) and space (the edge of the anticyclonic lens) provide an efficient mechanism of turbulent dissipation which cascades energy toward small scales in the frontal region.

For the uniform PV front configuration, small and intense cyclones are formed in a very short time ( $\sim 0.5T_f$ ) during the adjustment of a large scale anticyclonic front. By means of LIV, we visualize an horizontal cross-section of the sharp density gradient just below the free surface. The dynamical evolution of this sharp gradient is shown in figure 4. After the release of the bottomless cylinder the upper front experiences a rapid radial contraction. Due to the angular momentum conservation, this radial contraction generates at the same time a strong azimuthal shear flow. During this very initial stage, small scale perturbation growths at the edge of the front. Unlike the warm-core lens configuration, this instability leads to the formation of intense cyclones. The rapid formation of these structures, which are much smaller than the deformation radius, were not predicted by the standard scenario of adjustment and they could hardly be captured by standard numerical simulations which have limited spatial resolution. The laboratory experiment shows here a new mechanism of formation of small and intense cyclones within a large-scale synoptic front.

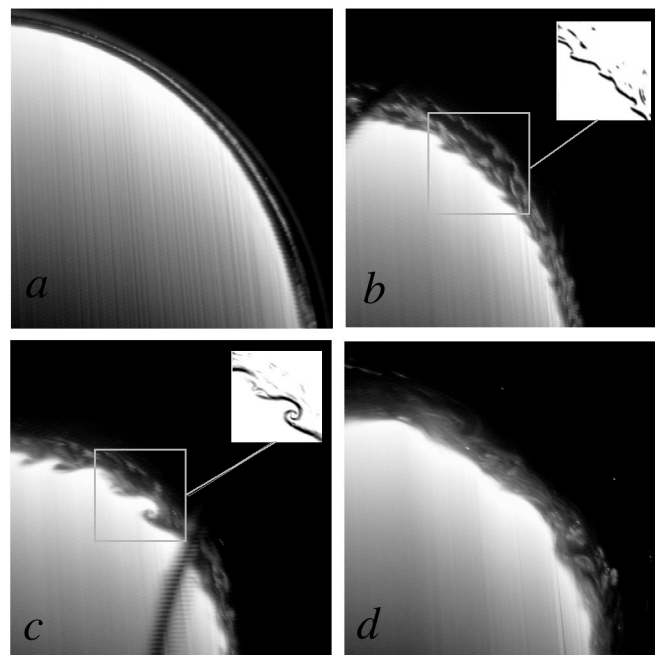


FIG. 4 – Small-scale instabilities during the geostrophic adjustment of a uniform PV front ( $Bu=0.14$ ) at  $t=0$  (a),  $t=0.25T_f$  (b),  $t=0.5T_f$  (c) and  $t=0.72T_f$  (d). Local image processing of edge front detection are shown in (b) and (c), the black pixels corresponds to high values of the intensity gradient.

## 6 Conclusions

Recent measurements techniques were used to investigate the geostrophic adjustment of density fronts. Several configurations were studied: warm core lens, cyclonic-anticyclonic PV patches and uniform PV front. According to the cases we studied we have shown that during this rapid adjustment toward a quasi-equilibrium state, an important part of the initial energy could be transferred to wave motion or dissipated by small-scale non-hydrostatic instabilities. In some specific case these transient instabilities could lead to the formation of intense and small-scale cyclones within a large-scale synoptic front. Nevertheless, a mean adjusted state is always reached after one or two inertial period. Outside the outcropping region, the PV conservation is robust and the standard Rossby adjustment predict correctly the mean adjusted state. Moreover, even if a strong wave activity is present in the initial region of unbalance, the time-averaged mean flow could nevertheless be adjusted. This experimental observation is in good agreement with the standard hypothesis of dynamical splitting between the fast and the slow component of motion. Besides, we have shown that the wave modes frequency is concentrated around the inertial frequency, and some anticyclonic structures exhibit sub-inertial oscillations corresponding to trapped modes.

## References

- Blumen, W. and Wu, R. 1995 Geostrophic adjustment: frontogenesis and energy conservation. *J. Phys. Oceanogr.*, **58**, 2180-2195.
- Bouruet-Aubertot, P. and Linden, P.F. (2002) The influence of the coast on the dynamics of upwelling fronts. Part I: Laboratory experiments. *Dyn. Atmos. Ocean.* **36**, pp 153-173.
- Kuo, A. C. and Polvani, L. M. (2000) Nonlinear geostrophic adjustment, cyclone/anticyclone asymmetry, and potential vorticity rearrangement. *Phys. Fluids* **12**, 1087-1100.
- Plougonwen, R. and Zeitlin, V. 2005 Lagrangian approach to geostrophic adjustment of frontal anomalies in a stratified fluid, *Geophys. Astrophys. Fluid Dyn.*, **99** (2), 101-135.
- Rossby, C. G. 1937 On the mutual adjustment of pressure and velocity distribution in simple current systems. *Int. J. Mar. Res.* **1**, 15-28.
- Rubino, A. and Brandt, P (2003) Warm-core eddies studied by laboratory experiments and numerical modeling. *J. Phys. Oceanogr.* **33**(2), pp 431-435.
- Stegner, A. Bouruet-Aubertot, P. and Pichon T. (2004) Nonlinear adjustment of density fronts. Part 1. The Rossby scenario and the experimental reality, *J. Fluid Mech.*, **502**, pp 335-360.
- Stegner, A. (2007) Experimental reality of geostrophic adjustment, Chapter 5 of *Edited Sciences on Advances in Nonlinear Science and Complexity* v.2 edited by V. Zeitlin, Elsevier.
- Thivolle-Cazat, E., Sommeria, J. and Galmiche, M. (2005) Baroclinic instability of two-layer vortices in laboratory experiments, *J. Fluid Mech.* **544**, 69-97.
- Ungarish, M., Hallworth, M. A. and Huppert, H.E. (2001) Axisymmetric gravity currents in a rotating system: Experimental and numerical investigations. *J. Fluid Mech.*, **447**, 1-29.
- Zeitlin, V. Reznik, G.M. and Ben Jelloul, M. (2003) Nonlinear theory of geostrophic adjustment. Part 2. Two-layer and continuously stratified primitive equations, *J. Fluid Mech.*, **491**, 207-228.